Rubio-López, A., Hoang, T., & Santiuste, C. (2016). Constitutive model to predict the viscoplastic behaviour of natural fibres based composites. Composite Structures, 155, 8-18

doi:https://doi.org/10.1016/j.compstruct.2016.08.001

Constitutive model to predict the viscoplastic behaviour of natural fibres based composites

A. Rubio-López

T. Hoang

C. Santiuste*

csantius@ing.uc3m.es

Department of Continuum Mechanics and Structural Analysis, University Carlos III of Madrid, Avda de la Universidad 30, 28911 Leganés, Madrid, Spain

*Corresponding author.

Abstract

The mechanical behaviour of traditional composites is usually assumed as linear-elastic up to failure. However, composites based on natural fibres are characterized by non-linear elasticity, viscous effects and plastic strains before failure. This study presents a rheological model to predict the viscoplastic behaviour of natural fibres based composites. The model was calibrated using a stress-strain curve and two relaxation tests for three different composites reinforced with flax, jute and cotton fibres. The model predicted successfully the behaviour of biocomposites loaded at different strain rates.

Keywords: Natural fibres; Rheological model; Viscoplasticity; Strain rate

1 Introduction

Traditional composites consist on the combination of synthetic fibres from mineral origin as glass or carbon fibres with oil-based polymer matrices as epoxy, polyethylene or polypropylene. In the last years, natural fibres (flax, cotton, sisal, jute, etc.) were introduced as potential substitutes of synthetic fibres in order to reduce the environmental impact of composites [1]. Few years ago, also vegetal origin polymers as polyhidroxybutyrate (PHB) or poly-lactic acid (PLA) were studied for their application as matrices to obtain a fully biodegradable composite, recyclable and with competitive mechanical properties [2]. The high specific mechanical strength of some fibres as well as their reduced costs make biocomposites suitable to preplace traditional composites for numerous applications [3].

Natural fibres as reinforcement of non-biodegradable plastics have already been used in automotive industry [4] and numerous publications studying these materials can be found [3–5]. However, the interest on fully biodegradable composites is growing as the authorities require ever more the use of recyclable materials due to environmental social concerns [6].

The disposal of theoretical models to predict the mechanical behaviour of biodegradable composites can help to get a better understanding of their performance and their use in industrial applications can increase. The mechanical behaviour of traditional composites has been widely studied [7–9]. Their behaviour can be usually assumed as linear-elastic up to failure [7], and the main objective in the development of predictive models is the implementation of accurate failure criteria [8] and the prediction of their energy absorption capability [9]. However, the development of constitutive models to predict the mechanical behaviour of biocomposites is an almost unexplored field. The results of experimental studies have shown viscoelastic and viscoplastic effects [10], thus traditional composites models assuming linear-elastic behaviour can be implemented in biocomposites only as a first approach [11].

The preliminary studies that have been initiated to predict the mechanical behaviour of natural fibres based composites can be divided into three different categories. The first category includes models for the prediction of the elastic properties and they are based on the rule of mixtures. The next step is the development of micromechanical models based on the reproducibility of a unit cell with FEM (finite element modelling), these models can be grouped in the second category. Finally, the third category includes constitutive models developed to consider the viscoplastic behaviour of biocomposites in a simplified mathematical formulation.

Numerous publications can be found in the first category, for example, Ihueza et al. [12] simulated the behaviour of polyester and natural fibre composites under multiaxial stress state. Facca et al. [13] developed a model to predict the elastic modulus of natural fibres reinforced thermoplastics. Virk et al. modelled the tensile properties of jute fibres [14] and predicted the elastic modulus and strength of natural fibre

composites [15]. These models are based in the prediction of the elastic properties, but they cannot include the strain rate dependency or the presence of permanent strains.

Regarding the micromechanical models, Andersons and Modniks [16] reproduced the tensile stress/strain behaviour of short fibre flax/epoxy composites. Sliseris et al. [17] also developed a micromechanical model based on the generation of fibres, bundles and fibre defects randomly with FEM to consider the fibre orientation, reproducing the stress/strain behaviour of short fibre and woven fabrics of flax reinforcing an epoxy matrix. Muttrand et al. [18] created a numerical model to reproduce randomly the cross-section geometry of flax fibres inside a flax/epoxy composite. Beakou and Charlet [19] simulated a flax bundle through a numerical model. These models are based on the definition of the fibre configuration, what means an overly high computational cost when implementing this in a macro mechanical FEM model.

Very few works can be found in the third category. Andersons et al. [20] developed a semiempirical tensor-linear model in order to predict the non-linear stress/strain behaviour of unidirectional flax/epoxy composites. Only the model proposed by Poilane et al. [10] can be considered a constitutive model considering the viscoelastic behaviour present in natural fibre composites. They developed a non-linear phenomenological model for flax/epoxy composites, based on rheological elements with eight parameters. The repetitive loading and unloading tensile tests on flax/epoxy composites with different yarn configurations were successfully predicted. However, this model was applied only to flax/epoxy composites, thus none model has been able to predict the viscoplastic behaviour of fully-biodegradable composites

In this work, a rheological model is introduced to define the viscoplastic behaviour of biocomposites. The model predicted accurately the viscoplastic behaviour of PLA based composites reinforced with three different woven fibres (flax, jute and cotton). One of the main goals of the present model is that it can be calibrated using only quasi-static tests; the influence of strain rate can be obtained from relaxation tests. Once the model is calibrated, it predicts the stress-strain curves obtained at different strain rates.

2 Experimental procedure

2.1 Materials

Three different woven fibres (flax, jute and cotton) with no chemical pre-treatments were acquired to verify the capability of the model to predict the mechanical behaviour of different biocomposites. Cotton and flax have 2 × 1 basket weave configuration while jute fabric configuration is plain. PLA matrix can be obtained from roots, sugarcane or corn starch polymerization [3]. For this study, PLA 10361D was acquired from Natureworks LLC, and it is defined as a biodegradable thermoplastic resin specifically aimed as a natural fibre binder. Fibres and matrix properties were studied in a previous work [21].

2.2 Manufacturing process

Biocomposites were produced by compression moulding process. First, three PLA layers and two woven fibres plies were alternatively stacked, then the laminate was place between two thermoheated plates, and pressure was applied by a universal testing machine. An optimization of the manufacturing process was performed as reported in [21], revealing that the optimum manufacturing parameters are 185 °C plates initial temperature, applying 8–16 MPa of pressure during 3 min after 2 min of preheating time. The fibre weight ratio was stated in 65% as studied by Ochi et al. [22]. The size of manufactured plates was 150 × 150 mm, while thicknesses were different for each raw material: 1.50 ± 0.05 mm for cotton, 1.15 ± 0.03 mm for jute and 1.27 ± 0.02 mm for flax composites.

Fabric and PLA plies were maintained in an oven under 95 °C during 30 min before the compression moulding processing to remove water content. All the materials were stored in stable constant conditions of 46% RH and 20 °C before and after the manufacturing process to control the environmental conditions influence.

2.3 Mechanical testing

An Instron 8516 universal testing machine was used to perform both tensile and relaxation tests. Manufactured plates were cut into 120 × 15 mm rectangular specimens. Cotton and flax 2 × 1 basket weave samples were oriented longitudinally.

Three different crosshead velocities were used for the tensile tests to obtain the stress-strain curves: 0.5 mm/min, 5 mm/min and 20 mm/min. The free length between clamping areas was established in 40 mm for all the tests, thus strain rates were $2.08 \cdot 10^{-4}$ s^{-1}, $2.08 \cdot 10^{-3}$ s^{-1} and $8.33 \cdot 10^{-3}$ s^{-1}.

Relaxation tests were performed imposing an initial displacement of the head with a 10 mm/s crosshead speed, leading to a strain rate equal to $2.5 \cdot 10^{-1}$ s^{-1}. This initial displacement was maintained until the recorded force was relaxed to a constant value.

3 Model description

Rheological models are based on the use of elastic, plastic and viscous elements [23] to determine the mechanical behaviour of a material and its temporal dependence under different loading conditions.

The model used in this work is defined with three branches in parallel, as shown in Fig. 1. In the first branch (a), the non-linear elastic behaviour of the material is defined through a Yeoh model [24], a phenomenological model based in rubber behaviour that defines the non-linear elastic behaviour using the strain energy density function. In the second branch (b), the viscous behaviour of the material is defined through a Maxwell model. Finally, in the third branch (c), the plasticity is introduced by a frictional analogy to the Maxwell model. Fig. 1 represents the scheme of the whole model, defined by only five elements.

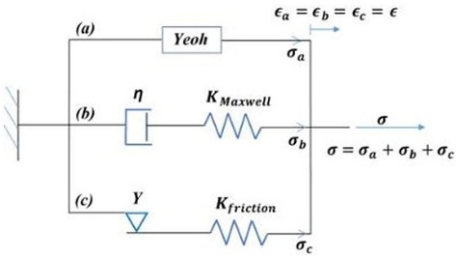

Fig. 1 Rheological model scheme. Branch (a) describes non-linear elasticity, branch (b) considers viscous effects and branch (c) includes plasticity.

3.1 Constitutive equations

Yeoh non-linear elastic model is based on incompressible materials, thus, the energy density function depends on the first invariant of the left Cauchy-Green deformation tensor in a cubic form, as Eq. (1) shows.

$$W = \sum_{i=1}^{3} C_i (I_1 - 3)^3 \tag{1}$$

where W is the strain energy density function, C_i represents elastic constants and I_1 is the first invariant. The first invariant is the trace of the left Cauchy-Green deformation tensor ($B = FF^T$, being F the deformation gradient tensor and B the left Cauchy-Green deformation tensor). Considering incompressibility and uniaxial extension, the stretches ($\lambda = \epsilon + 1$) in the three principal directions can be related as $\lambda_1 \cdot \lambda_2 \cdot \lambda_3 = 1$ and $\lambda_2 = \lambda_3$, thus

$$I_1 = \lambda_1^2 + \lambda_2^2 + \lambda_3^2 = \lambda^2 + \frac{2}{\lambda} \tag{2}$$

Considering the left Cauchy-Green deformation tensor expressed as $B = \lambda^2 \cdot n_1 \times n_1 + \frac{1}{\lambda} \cdot (n_2 \times n_2 + n_3 \times n_3)$ and uniaxial extension, orienting the principal stretches with the coordinated basis vectors, the stress in the principal direction results: $\sigma_{11} = -p + 2 \cdot \lambda^2 \frac{\partial W}{\partial I_1}$ and $\sigma_{22} = \sigma_{33} = -p + \frac{2}{\lambda} \frac{\partial W}{\partial I_1} = 0$, thus $p = \frac{2}{\lambda} \frac{\partial W}{\partial I_1}$ and

$$\sigma_{11} = 2 \cdot \left(\lambda^2 - \frac{1}{\lambda} \right) \frac{\partial W}{\partial I_1} \tag{3}$$

The derivate of strain energy density function can be obtained from Eq. (1):

$$\frac{\partial W}{\partial I_1} = \sum_{i=1}^{3} i \cdot C_i (I_1 - 3)^{i-1} \tag{4}$$

Introducing Eq. (2) in Eq. (4) and Eq. (4) in Eq. (3), stress can be expressed as a function of strain for the non-linear Yeoh model under uniaxial extension, Eq. (5):

$$\sigma_{Yeoh} = \frac{2\epsilon(3+\epsilon(3+\epsilon))((1+\epsilon)^2 C_1 + \epsilon^2(3+\epsilon)(2(1+\epsilon)C_2 + 3\epsilon^2(3+\epsilon)C_3)}{(1+\epsilon)^2} \quad \sigma_{Yeoh} = \frac{2\,\epsilon\left(3+\epsilon\left(3+\epsilon\right)\right)\left((1+\epsilon)^2 C_1 + \epsilon^2\left(3+\epsilon\right)\left(2\left(1+\epsilon\right)C_2 + 3\epsilon^2\left(3+\epsilon\right)C_3\right)\right)}{(1+\epsilon)^2} \tag{5}$$

where C_1, C_2 and C_3 are three elastic constants.

The second branch (b) function is to introduce the viscous effects, thus a Maxwell model was used, whose behaviour is described by Eq. (6). The Maxwell model behaviour is given by a spring and a dashpot in series, thus the stress is the same in both elements ($\sigma_{dashpot} = \sigma_{spring} = \sigma$) and the total strain is the sum of the spring and dashpot strains ($\epsilon_{dashpot} + \epsilon_{spring} = \epsilon$). The constitutive equation of the Maxwell model is obtained including the spring definition $\sigma = K \cdot \epsilon$ (K is the spring's constant) and the dashpot equation $\sigma = \eta \cdot \frac{d\epsilon}{dt}$ (?? is the dashpot constant) in the strain-rate equation, $\dot{\epsilon}_{dashpot} + \dot{\epsilon}_{spring} = \dot{\epsilon}$, yielding:

$$\dot{\sigma}_{Maxwell} + \frac{K}{\eta} \cdot \sigma_{Maxwell} = K \cdot \dot{\epsilon} \tag{6}$$

Finally, branch (c) introduces plasticity through a spring and a frictional element in series. These two elements produce a frictional analogy to the Maxwell model to define a plastic behaviour. The model stiffness is dominated by the spring element until the frictional element is activated, the role of the frictional element is to stablish a limit for the stress. Thus, the definition of the stress/strain relationship for the frictional branch is given in two sections as shown in Eq. (7), before and after the yield strain is reached ($\varepsilon_y = Y/K_{Friction}$).

$$\begin{aligned} &if\ \varepsilon < \varepsilon_y \rightarrow \sigma_{Friction} = K_{friction} \cdot \epsilon \\ &\quad if\ \varepsilon \geqslant \varepsilon_y \rightarrow \sigma_{Friction} = Y \end{aligned} \tag{7}$$

Being defined the constitutive equation of each branch, the constitutive equation of the global model is given by Eq. (8).

$$\sigma = \sigma_{Yeoh} + \sigma_{Maxwell} + \sigma_{Friction} \tag{8}$$

3.2 Stress-strain response

The solution of the constitutive equations for the tensile test is presented in this section. The three branched can be solved separately imposing initial conditions: $\epsilon(0) = 0$ and $\sigma(0) = 0$, and imposing a constant strain rate. The solution of the Maxwell model differential equation is:

$$\sigma_{Maxwell-Tensile} = \dot{\epsilon} \cdot \eta \cdot \left(1 + e^{-\frac{K_{Maxwell}}{\eta} \cdot t}\right) \tag{9}$$

The solution for the Yeoh and the friction branches are independent of the strain rate, thus the solution can be found replacing $\epsilon = \dot{\epsilon} \cdot t$ in Eq. (5) and Eq. (7). The solution of the global model, Eq. (8), for different strain rates is shown in Fig. 2.

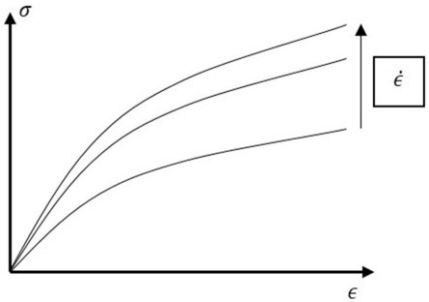

Fig. 2 Tensile tests strain rate dependence. Stress-strain curves obtained for different strain rates.

3.3 Relaxation response

In relaxation tests an initial strain is imposed and maintained with time ($\epsilon = \epsilon_0$ and $\dot{\epsilon} = 0$). The initial strain is considered to be applied instantaneously, thus infinity strain rate can be assumed, see Fig. 3a. Therefore, the dashpot of the Maxwell model can be considered initially blocked and the first value of the stress is controlled by the spring $\sigma(0) = K_{Maxwell} \cdot \epsilon_0$. On the other hand, the dashpot will be relaxed during the test and the final value of the stress in the Maxwell model is zero. The solution of ODE Eq. (6) is:

$$\sigma_{Maxwell-Relaxation} = K_{Maxwell} \cdot \epsilon_0 \cdot e^{-\frac{K_{Maxwell}}{\eta} \cdot t} \tag{10}$$

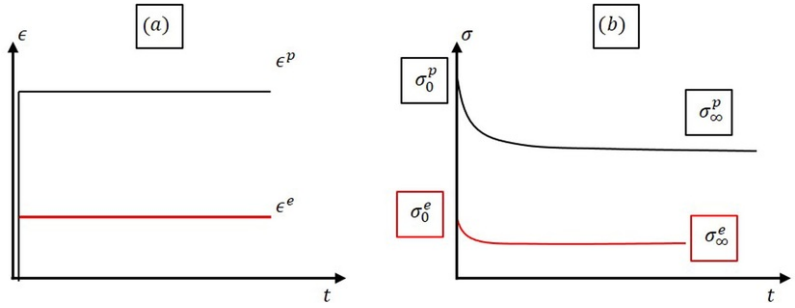

Fig. 3 Relaxation test description. (a) Strain vs. time curves. (b) Stress vs. time curves.

The solutions of the Yeoh and the frictional elements are time independent. Thus solution can be obtained introducing $\epsilon = \epsilon_0$ in Eqs. (5) and (7), respectively. The stress remains constant in these two elements as the strain does. The global response of the model in the relaxation tests is shown in Fig. 3b. Two different tests are shown in Fig. 3, viscoelastic and viscoplastic, denominated by superindexes "*e*" and "*p*" respectively. The strain imposed in the viscoelastic relaxation test is lower than the yield strain while the strain imposed in the viscoplastic relaxation test is higher.

3.4 Model calibration and validation

Seven parameters are used to define the present model: C_1, C_2, and C_3 are the elastic constant of the Yeoh model, $K_{Maxwell}$ and η are the spring and dashpot constants of the Maxwell model, and $K_{friction}$ and Y are the friction model parameters. Three different tests were conducted to calibrate these parameters for each material: viscoelastic and viscoplastic relaxation tests (Fig. 3a and b) and a quasi-static tensile test (Fig. 2). Two tensile tests were conducted at higher strain rates to validate the ability of the model to predict the viscoplastic behaviour of biocomposites.

Four values can be obtained from relaxation tests to calibrate the model. The initial stress of the viscoelastic test (σ_0^e) is defined by Eq. (11) while the final stress (σ_∞^e) is given by Eq. (12), being ϵ^e the imposed strain. The initial and final stresses of the viscoelastic relaxation test are shown in Eqs. (13) and (14) respectively, being ϵ^p the imposed strain.

$$\sigma_0^e = \sigma_{Yeoh}(\in^e) + (K_{friction} + K_{Maxwell}) \cdot \epsilon^e, \quad \textbf{(11)}$$

$$\sigma_\infty^e = \sigma_{Yeoh}(\in^e) + K_{friction} \cdot \epsilon^e \quad \textbf{(12)}$$

$$\sigma_0^p = \sigma_{Yeoh}(\in^p) + Y + K_{Maxwell} \cdot \epsilon^e \quad \textbf{(13)}$$

$$\sigma_\infty^p = \sigma_{Yeoh}(\epsilon^p) + Y. \quad \textbf{(14)}$$

The values of $K_{friction}$, $K_{Maxwell}$, and Y can be obtained as a function of Yeoh parameters using Eqs. (11)-(13). Yeoh parameters, C_1, C_2, C_3, were fitted through an adjustment with least squared applied to a quasi-static tensile tests to obtain the stress-strain curve. Finally, dashpot parameter (η) was calibrated with the relaxation tests by least squared fit considering the viscoelastic and viscoplastic tests curvatures.

Eq. (14) was not used for the model calibration, for this reason σ_∞^p was used for validation. Additionally, two stress-strain curves obtained at higher strain rates were used to validate the model. Therefore, a great coherence is obtained as the model parameters were calibrated with a set of tests and different tests were used for validation.

4 Results and discussion

4.1 Experimental results

The results of the tensile tests conducted to obtain three stress-strain curves at different strain rates are shown in Fig. 4. The stiffness and the strength of flax composites are much higher than that of jute and cotton composites. The nonlinearity of cotton composites is clearer than in the other materials, there is a great difference between the slope of the stress-strain curves after and before the yield point.

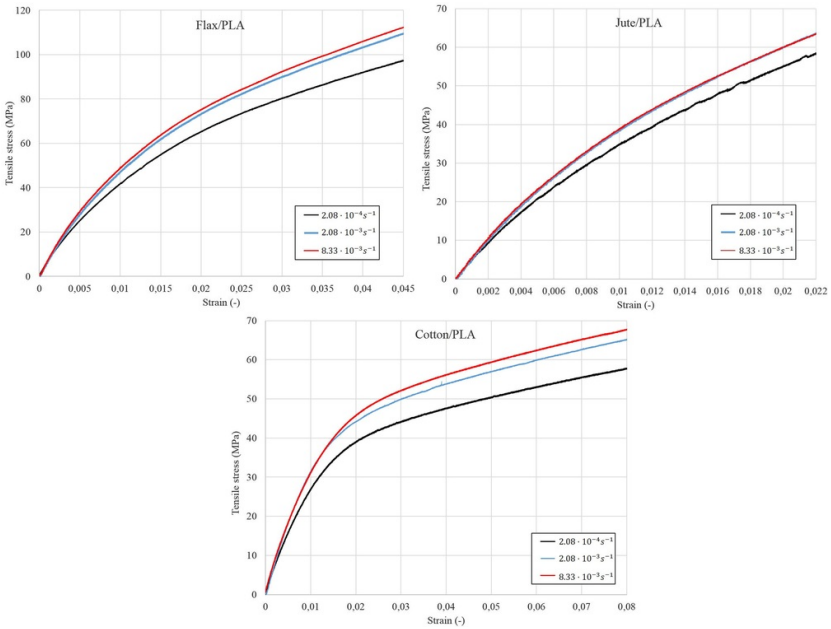

Fig. 4 Tensile tests conducted at different strain rates in flax, jute and cotton composites.

The viscous effects can be observed in the three materials because the stiffness increases with strain rate, but the influence of strain rate is lower in jute composites. In flax and cotton composites the stresses always increase with strain rate. However, in jute composites stresses increase when strain rate rise from 2.08×10^{-4} s^{-1} to 2.08×10^{-3} s^{-1}, but the curves for strain rates of 2.08×10^{-3} s^{-1} and 8.33×10^{-3} s^{-1} are overlapped. The stiffness increment observed in flax/PLA composites in similar to that reported by Polilâne et al. [10] in flax/epoxy composites, thus the viscous effects can probably be attribute to the mechanical behaviour of fibres.

The values of the imposed strains of the relaxation tests were selected from the stress-strain curves shown in Fig. 4. The elastic and plastic strains were chosen to conduct relaxation tests before and after the yield point, the values of the strains are shown in Table 1. Fig. 5 shows the relaxation results for each material, comparing viscoelastic with viscoplastic behaviour. In the three materials, viscoplastic tests needed more time to get a stable value of the final stress than viscoelastic tests. Cotton needed more time to get stable than flax while flax needed more time than jute. The initial and final stresses of each test are summarized in Table 1.

Table 1 Relaxation tests results: initial and final stresses.

	Flax/PLA	Cotton/PLA	Jute/PLA
Elastic strain (–)	0.0025	0.0025	0.00175
Plastic strain (–)	0.025	0.025	0.0125
σ_0^e (MPa)	14.2 ± 0.3	8.9 ± 0.1	9.3 ± 0.4
σ_∞^e (MPa)	11.7 ± 0.4	7.2 ± 0.2	8.2 ± 0.2
σ_0^p (MPa)	81.1 ± 2.2	42.0 ± 1.5	41.9 ± 0.5
σ_∞^p (MPa)	52.6 ± 1.5	24.5 ± 0.7	32.3 ± 1.0

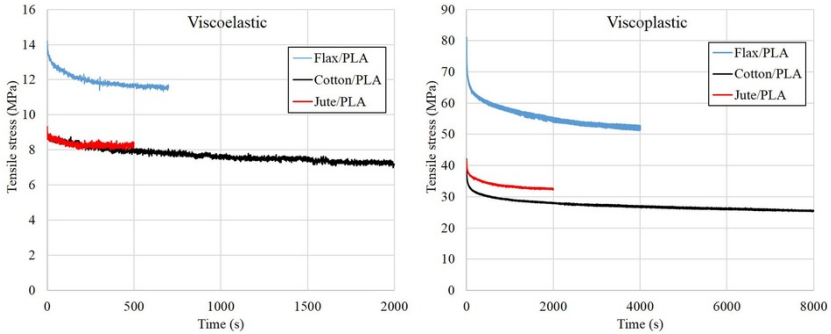

Fig. 5 Viscoelastic (a) and viscoplastic (b) relaxation tests results for flax/PLA, cotton/PLA, jute/PLA.

4.2 Model calibration

The results of relaxation tests and the stress-strain curves obtained at a strain rate of 2.08×10^{-4} s^{-1} were used to calibrate the model for the three materials. The values of the parameters calibrated are summarized in Table 2.

Table 2 Model parameters fitted for flax/PLA, jute/PLA and cotton/PLA biocomposites.

Parameter	Flax/PLA	Jute/PLA	Cotton/PLA
$K_{Maxwell}$ (Pa)	$1.08 \cdot 10^{9}$	$6.86 \cdot 10^{8}$	$6.40 \cdot 10^{8}$
$K_{friction}$ (Pa)	$2.58 \cdot 10^{9}$	$2.15 \cdot 10^{9}$	$2.71 \cdot 10^{9}$
η (Pa s)	$2.30 \cdot 10^{11}$	$6.14 \cdot 10^{10}$	$5.19 \cdot 10^{11}$
Y (Pa)	$1.23 \cdot 10^{7}$	$4.87 \cdot 10^{6}$	$2.36 \cdot 10^{7}$
C_1 (Pa)	$3.38 \cdot 10^{8}$	$4.14 \cdot 10^{8}$	$2.16 \cdot 10^{7}$
C_2 (Pa)	$-1.81 \cdot 10^{10}$	$-2.76 \cdot 10^{10}$	$-1.63 \cdot 10^{9}$
C_3 (Pa)	$6.56 \cdot 10^{11}$	$2.08 \cdot 10^{8}$	$2.15 \cdot 10^{10}$

A comparison between the experimental data and the model predictions with the fitted parameters is shown in Figs. 6–8 for flax, jute and cotton composites respectively. In each figure, the *a* and *b* graphs represents the viscoelastic and viscoplastic relaxation tests, where $K_{friction}$, $K_{Maxwell}$, η and Y were fitted, while *c* graph shows the stress/strain test where C_1, C_2 and C_3 parameters were calibrated through a least squares fitting.

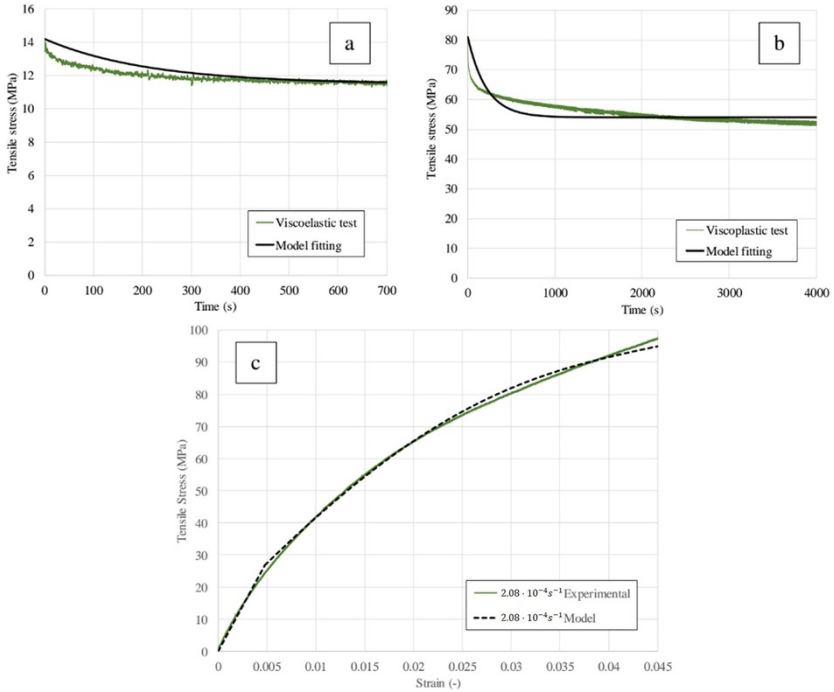

Fig. 6 Model parameters calibration of flax/PLA composites. (a) Viscoelastic relaxation test. (b) Viscoplastic relaxation test. (c) Stress-strain curve.

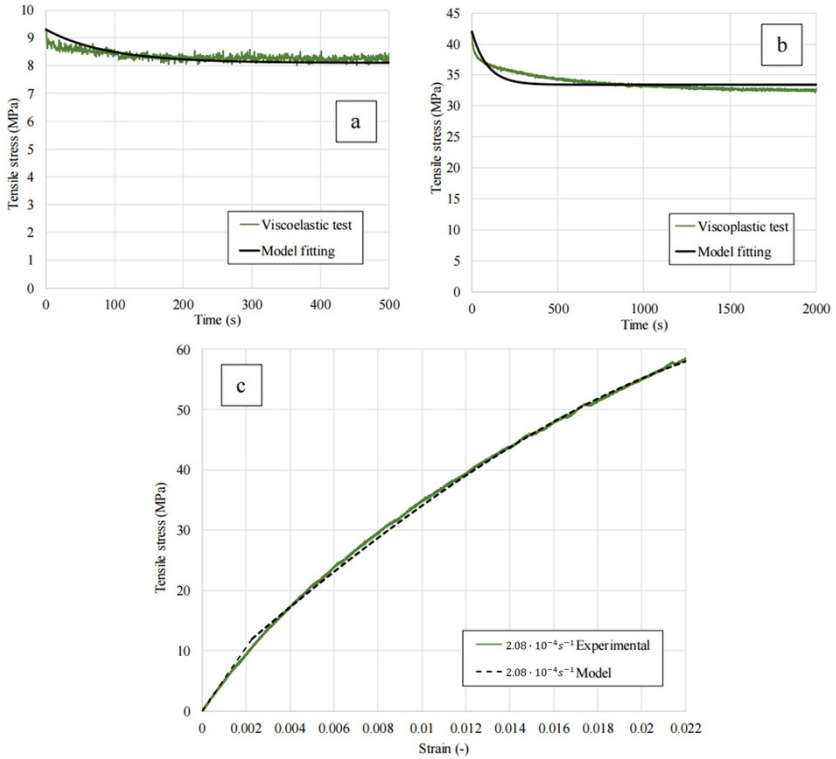

Fig. 7 Model parameters calibration of jute/PLA composites. (a) Viscoelastic relaxation test. (b) Viscoplastic relaxation test. (c) Stress-strain curve.

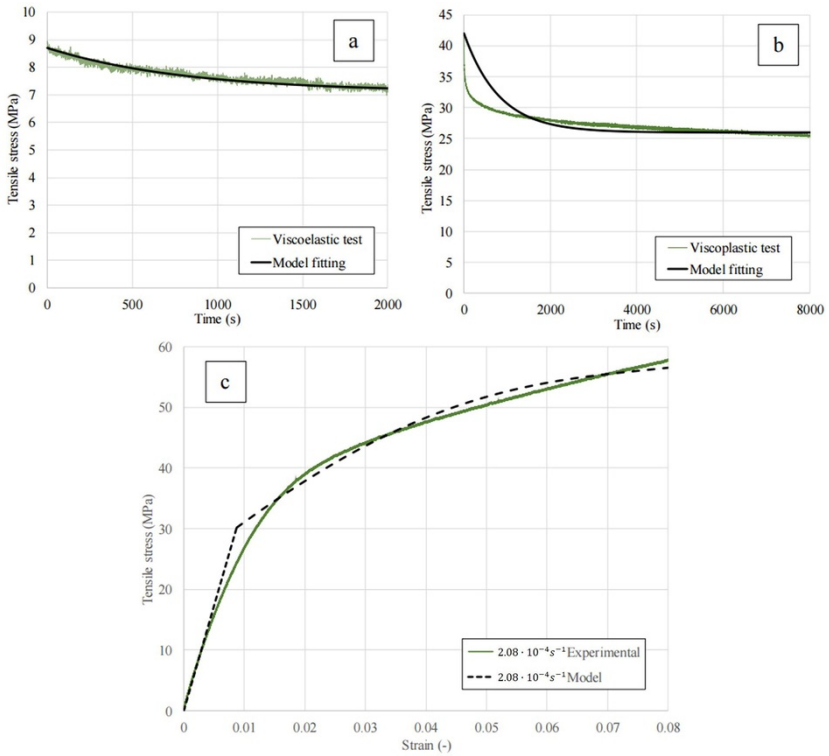

Fig. 8 Model parameters calibration of cotton/PLA composites. (a) Viscoelastic relaxation test. (b) Viscoplastic relaxation test. (c) Stress-strain curve.

4.3 Model validation

The first data used to validate the model were the final stress obtained in the viscoplastic relaxation tests (σ_{∞}^{p}). Table 3 includes the experimental data and the model predictions for the three materials. An excellent agreement between predictions and experiments can be observed, being the maximum error lower than 6%.

Table 3 Comparison between experimental and predicted final stress in viscoplastic relaxation tests (σ_{∞}^{p}).

	Flax/PLA	Cotton/PLA	Jute/PLA
σ_{∞}^{p} Experimental (Mpa)	52.6	24.5	32.3
σ_{∞}^{p} Model, Eq. (13) (Mpa)	54	26	34
Error (%)	2.6	5.8	5.0

Moreover, the tensile tests conducted at strain rates of $2.08{\cdot}10^{-3}$ s^{-1} and $8.33{\cdot}10^{-3}$ s^{-1} were used to validate the accuracy of the model in the prediction of the strain rate influence on stress-strain curves. Figs. 9–11 show the comparison between experimental data and predicted stress-strain curves for flax, jute and cotton composites. A reasonable agreement between the predictions and the experiments obtained, thus the model can be considered validated. The model predicts the influence of strain rate leading to an increase of the stiffness according to experimental results. It should be noticed that the model was calibrated using a single tensile test at a single strain rate, moreover the influence of strain rate is different in each material as it was explained before.

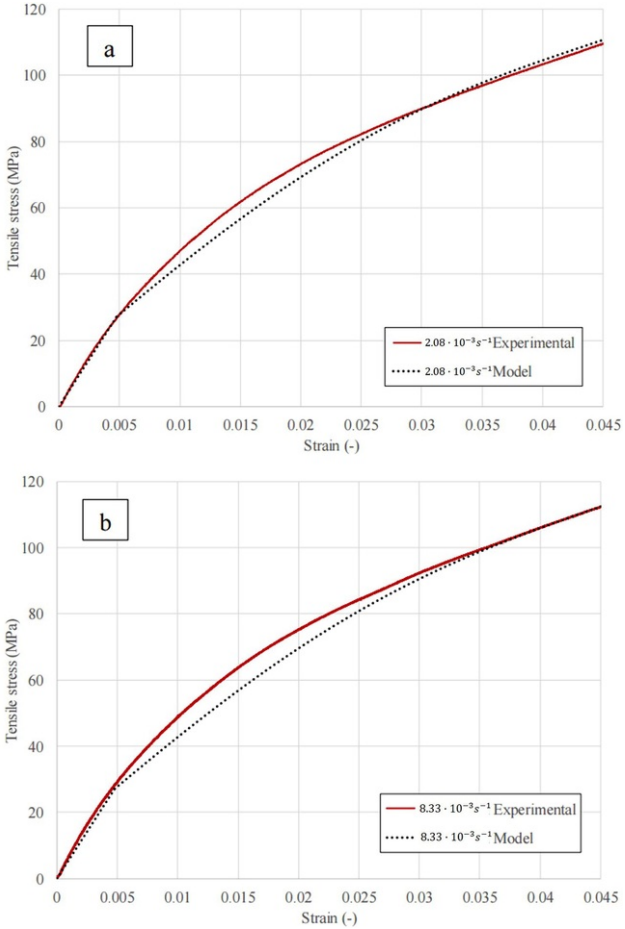

Fig. 9 Tensile tests conducted on flax/PLA composite at strain rates of $2.08{\cdot}10^{-3}$ s^{-1} and $8.33{\cdot}10^{-3}$ s^{-1}. Experimental results and model predictions.

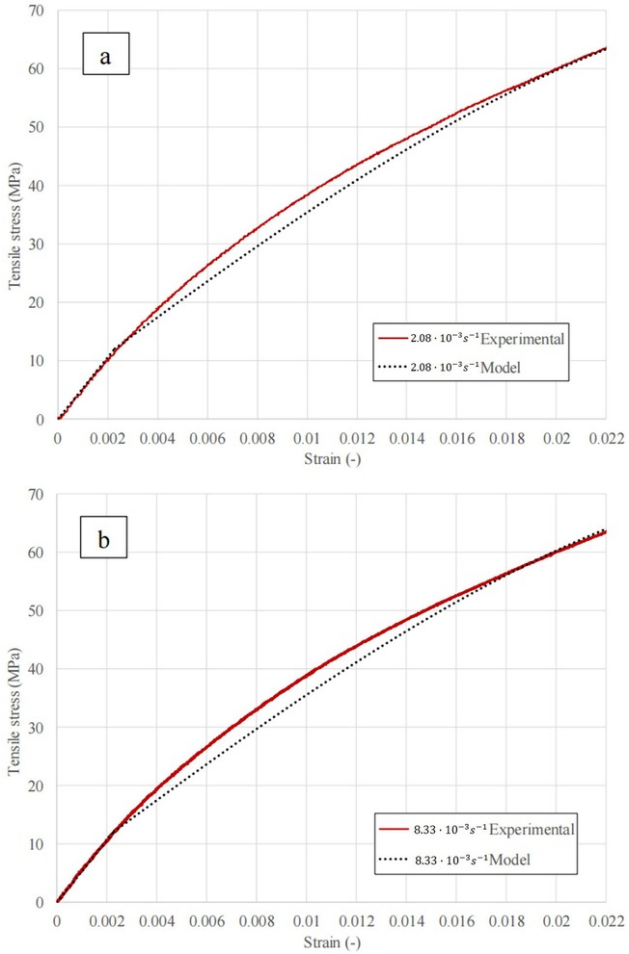

Fig. 10 Tensile tests conducted on jute/PLA composite at strain rates of $2.08{\cdot}10^{-3}$ s^{-1} and $8.33{\cdot}10^{-3}$ s^{-1}. Experimental results and model predictions.

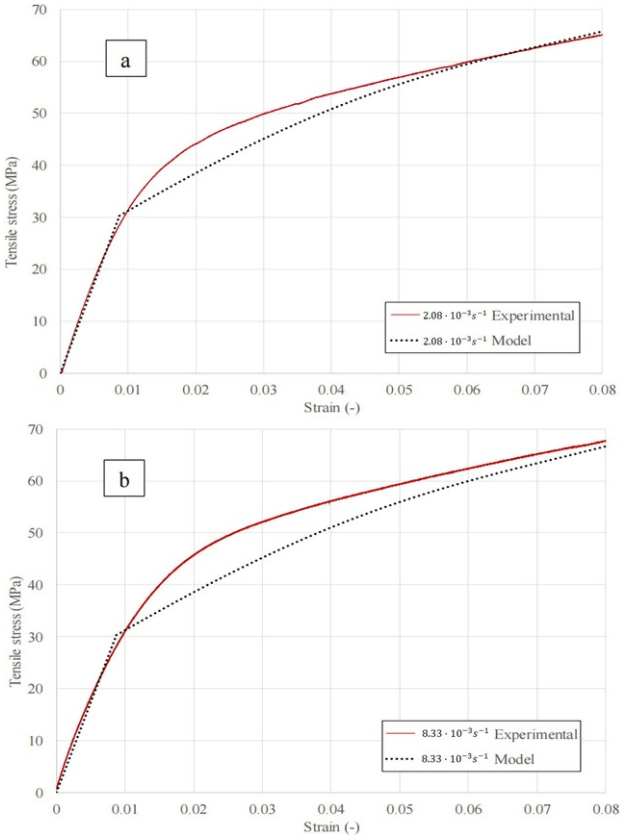

Fig. 11 Tensile tests conducted on cotton/PLA composite at strain rates of $2.08{\cdot}10^{-3}$ s^{-1} and $8.33{\cdot}10^{-3}$ s^{-1}. Experimental results and model predictions.

Nevertheless, the model accuracy is not perfect. The results with flax and jute composites show a better prediction capacity than with cotton. One of the reasons is that the friction branch controls the predicted yield strain, thus it is independent on strain rate. This hypothesis can be assumed for flax and jute composites according to experimental results. However, the yield strain in cotton composites experiences a slightly increase with strain rate as it was observed in experimental tests.

5 Conclusions

A constitutive model for fully biodegradable composites was developed for the first time. The model, based on rheological elements, includes the consideration of non-linear elastic behaviour, viscous effects and plastic strains. The model was successfully validated for three different biocomposites: flax/PLA, jute/PLA, and cotton/PLA woven laminates.

It should be noticed that the model was calibrated for each material using two relaxation tests and the stress-strain curve obtained at a single strain rate. The model predicted with a reasonable accuracy the influence of strain rate, the predicted stress-strain curves at higher strain rates were in agreement with experimental results. All the materials experience an increment in the stiffness with strain rate, but this effect was higher in flax and jute composites than in cotton laminates. The model predicted this difference between materials even when it was calibrated using only relaxation tests.

One of the main goals of the present model is that the model was validated for three different materials, what means that the model can help to bring some light to the physics behind the viscoplastic behaviour of biocomposites. This is only the first attempt to develop a constitutive model for fully-biodegradable material but some hypotheses are proposed:

1- The plastic strains can be accurately predicted with a single friction element. This means that the yield point can be associated to a value of strain that initiates the plastic behaviour. One of the most probable reasons is the friction between

fibres inside the yarns. The plastic behaviour of the matrix is an alternative explanation but it can be neglected due to the great differences in the values of yield strain for composites reinforced with different fibres.

2- The viscous effects can be attributed to fibres behaviour. The influence of matrix can be neglected again because the viscous effects are higher in the composites reinforced with stiffer fibres. Moreover, the influence of strain rate on the stiffness of flax/PLA composites is similar to that reported by other authors in flax/epoxy composites.

3- The non-linear elastic behaviour can be probably explained by a combination of woven fibres and matrix.

These hypotheses can be considered the starting point for future research in this field. The present promising results can lead to get a better understanding of the mechanical behaviour of biocomposites and to increase their use in industrial applications to replace mineral fibres and oil-based polymer matrices.

Acknowledgments

Authors gratefully acknowledges the support of Spanish Ministry of Economy under the project DPI2013-43994-R.

References

[1] A.K. Mohanty, M. Misra and L.T. Drzal, (Eds.), *Natural fibers, biopolymers, and biocomposites,* 2005, CRC Press.

[2] P. Wambua, J. Ivens and I. Verpoest, Natural fibres: can they replace glass in fibre reinforced plastics?, *Compos Sci Technol* **63** (9), 2003, 1259–1264.

[3] K.G. Satyanarayana, G.G.C. Arizaga and F. Wypych, Biodegradable composites based on lignocellulosic fibers – an overview, *Prog Polym Sci* **34** (9), 2009, 982–1021.

[4] G. Koronis, A. Silva and M. Fontul, Green composites: a review of adequate materials for automotive applications, *Compos Part B* **44** (1), 2013, 120–127.

[5] M.J. John and S. Thomas, Biofibres and biocomposites, *Carbohydr Polym* **71** (3), 2008, 343–364.

[6] European Union, The Directive 2000/53/EC of the European Parliament and of the Council of 18 September 2000 on end-of-life vehicles, *OJ L* **269**, 2000, 34–49.

[7] C. Santiuste, O.T. Thomsen and Y. Frostig, Thermo-mechanical load interactions in foam cored axi-symmetric sandwich circular plates-High-order and FE models, *Compos Struct* **93** (2), 2011, 369–376.

[8] C. Santiuste, S. Sánchez-Sáez and E. Barbero, A comparison of progressive-failure criteria in the prediction of the dynamic bending failure of composite laminated beams, *Compos Struct* **92** (10), 2010, 2406–2414.

[9] X. Soldani, C. Santiuste, A. Muñoz-Sánchez and M.H. Miguélez, Influence of tool geometry and numerical parameters when modeling orthogonal cutting of LFRP composites, *Compos Part A* **42** (9), 2011, 1205–1216

[10] C. Poilâne, Z.E. Cherif, F. Richard, A. Vivet, B.B. Doudou and J. Chen, Polymer reinforced by flax fibres as a viscoelastoplastic material, *Compos Struct* **112** (1), 2014, 100–112.

[11] A. Rubio-López, A. Olmedo and C. Santiuste, Modelling impact behaviour of all-cellulose composite plates, *Compos Struct* **122**, 2015, 139–143.

[12] C.C. Ihueze, C.E. Okafor and C.I. Okoye, Natural fiber composite design and characterization for limit stress prediction in multiaxial stress state, *J King Saud Univ Eng Sci* **27** (2), 2013, 193–206.

[13] A.G. Facca, M.T. Kortschot and N. Yan, Predicting the elastic modulus of natural fibre reinforced thermoplastics, *Compos Part A* **37**, 2006, 1660–1671.

[14] A.S. Virk, W. Hall and J. Summerscales, Modelling tensile properties of jute fibres, *Mater Sci Technol* **27** (1), 2011, 458–460.

[15] A.S. Virk, W. Hall and J. Summerscales, Modulus and strength prediction for natural fibre composites, *Mater Sci Technol* **28** (7), 2012, 864–871.

[16] J. Modniks and J. Andersons, Modeling the non-linear deformation of a short-flax-fiber-reinforced polymer composite by orientation averaging, *Compos Part B* **54**, 2013, 188–193.

[17] J. Sliseris, L. Yan and B. Kasal, Numerical modelling of flax short fibre reinforced and flax fibre fabric reinforced polymer composites, *Compos Part B* **89**, 2016, 143–154.

[18] C. Mattrand, A. Béakou and K. Charlet, Numerical modeling of the flax fiber morphology variability, *Compos Part A* **63**, 2014, 10–20.

[19] A. Beakou and K. Charlet, Mechanical properties of interfaces within a flax bundle-Part II: numerical analysis, *Int J Adhes Adhes* **43**, 2013, 54–59.

[20] J. Andersons, J. Modniks and E. Spārniņš, Modeling the nonlinear deformation of flax-fiber-reinforced polymer matrix laminates in active loading, *J Reinf Plast Compos* **34** (3), 2015, 248–256.

[21] A. Rubio-López, A. Olmedo, A. Diaz-Alvarez and C. Santiuste, Manufacture of compression moulded PLA based biocomposites: a parametric study, *Compos Struct* **131**, 2015, 995–1000.

[22] S. Ochi, Mechanical properties of kenaf fibers and kenaf/PLA composites, *Mech Mater* **40** (4), 2008, 446–452.

[23] A Persson and F. Karlsson, Modelling non-linear dynamics of rubber bushings-parameter identification and validation, [Ph.D. thesis]2003, Lund University.

[24] O.H. Yeoh, Some forms of the strain energy function for rubber, *Rubber Chem Technol* **66** (5), 1993, 754–771.